Kinetic study of quantum two-stream instability by Wigner approach

Jiong-Hang Liang ◉,[1] Tian-Xing Hu ◉,[1] D. Wu ◉,[1,2,*] and Zheng-Mao Sheng ◉[1,†]

[1]*Institute for Fusion Theory and Simulation, Department of Physics, Zhejiang University, 310027 Hangzhou, China*
[2]*Collaborative Innovation Center of IFSA, Shanghai Jiao Tong University, Shanghai 200240, China*

Classical plasma are typically of low density and/or high temperature. Two of its basic properties are Landau damping and two-stream instabilities. When increasing the plasma density, quantum effects appear and beam-plasma interactions show behavior different from the classical cases. We revisit Landau damping and two-stream instabilities under conditions when quantum hydrodynamic and quantum kinetic theory can be applied, the latter accounting for wave-particle interactions. We find that the instability growth rate behaves as pure two-stream instability without Landau damping when the countering stream velocity exceeds a certain threshold, which differs from the classical case.

I. INTRODUCTION

High energy density physics (HEDP), especially the warm dense matter (WDM) or hot dense matter (HDM) regimes [1–5], has received attention in recent years. WDM or HDM widely exists in inertial confinement fusion [6–8], and (laboratory) astrophysics studies [9–11], with temperatures of $1 \sim 100$ eV and density of $0.1 \sim 10$ solid densities. However, due to the significantly higher temperatures when compared with the condensed matter state and high densities, many properties of WDM or HDM are not well studied.

Two basic properties of a plasma are Landau damping and two-stream instability. Landau damping [12] defines "kinetic" effects of the kind of wave-particle interaction, while two-stream instability represents the excitation of oscillations of charged particles in plasma. In most cases, the two-stream instability cannot be treated as a pure fluid instability since plasmas in reality always have velocity distributions departing from thermal equilibrium, which means that the kinetic effects exist. Although extensively investigated in ideal plasmas [13], under the WDM or HDM regime, such properties are seldom studied. In this case, instabilities differ from classical plasmas in two respects: (1) the equilibrium distribution function becomes Fermi-Dirac instead of Maxwellian; (2) the quantum mechanical feature, i.e., the wave-like behavior, of the single-particle wave duality becomes relevant.

An investigation of dense plasma starts from the pioneering works of Bohm and Pines [14,15] who utilized the random phase approximation (RPA) approach in calculating the dynamic response of degenerate plasmas. Under classical plasmas, the RPA approach reproduces the Bohm-Gross wave (BG) with Landau damping, and for degenerate plasmas, one obtains its quantum counterparts. Bonitz summarized the quantum effects in three-dimensional systems [16–19].

Vladimirov gave an analytical description of collisonless quantum plasma [20]. Manfredi and Haas established the quantum hydrodynamics (QHD) theory [21]. Ren and Wu discussed the multistream instability in quantum magnetized hot plasmas based on QHD [22]. Haas gave the fluid expression form of quantum two-stream instability, proved that the effective Schrodinger-Poisson system (QHD) is a good approximation to the complete Wigner-Poisson system (QKT) for long wavelengths, analyzed the nonlinear process via QHD, and revised QHD under consideration of exchange-correlation effects [23–25]. Kull discussed the quantum two-stream instability with exchange interaction via time-dependent two-coupled Schroedinger equations [26]. Akbari-Moghanjoughi compared the difference between fluid approximation and the dynamic limit of the Wigner-Poisson equation [27–29]. Son discussed the difference between classical and quantum cases through the Lindhard description and gave a conclusion that the kinetic approach was more accurate than QHD in studying two-stream instability [30].

However, most of these finished works are based on QHD, which ignores the wave-particle interactions. Therefore, they are not suitable for extension to the high-energy density regime where high temperatures can significantly affect wave-particle interactions and instabilities. The Lindhard description in [30] applies to Fermi gas at zero temperature and does not consider the temperature effects in detail.

In this paper, we revisit the Landau damping and two-stream instability by using both QHD and QKT theories. The quantum Landau damping and two-stream instabilities are here revisited at both the low temperature limit and WDM regions by using quantum hydrodynamic and quantum kinetic theories, with the later taking into account wave-particle interactions. WDM typically involves other nonideal effects, such as exchange-correlation effects, collision effects, and so on. In this paper, we apply an ideal Fermi-distribution based Wigner approach to simplify research in the high energy density regime. The similarity and discrepancy of the damping rate of Langmuir Wave between high energy density and

---

*dwu.phys@zju.edu.cn
†zmsheng@zju.edu.cn

classical plasmas are significantly compared and explained. Specifically, we find the plasma growth rate behaves as pure two-stream instability without Landau damping when the countering velocity exceeds a certain threshold, which is different from the classical case.

The article is organized as follows. In Sec. II, we give a brief introduction to QKT and QHD and summarize the previous results of two-stream instability under the QHD model. In Sec. III, we take the Lindhard function [31] and give the influence of quantum Landau damping on the dispersion relation, and then we study the property of quantum plasma depending on the system density and temperature. In Sec. IV, we consider the two-stream instability by using QKT theory, and give an explanation for the theoretical difference with the QHD model. Finally, we compare the effects of quantum dissipative instability under different system parameters. A summary and discussion are given in Sec. IV.

II. BRIEF REVIEW OF QKT AND QHD

We here give a brief introduction of QKT and QHD. Following the introduction, the existing work on two-stream instabilities based on QHD is also introduced.

A. Quantum kinetic theory

Quantum kinetic theory (QKT) [32] starts from the Wigner function [33]

$$\left(\frac{\partial}{\partial t} + \frac{\mathbf{p} \cdot \nabla_{\mathbf{R}}}{m}\right) f(\mathbf{p}, \mathbf{R}, t) = \frac{1}{i\hbar} \iint \frac{d\mathbf{r} d\mathbf{p}'}{(2\pi\hbar)^3} \exp\left(\frac{i(\mathbf{p} - \mathbf{p}') \cdot \mathbf{r}}{\hbar}\right) [U_{\text{eff}}(\mathbf{R} + \mathbf{r}/2, t) - U_{\text{eff}}(\mathbf{R} - \mathbf{r}/2, t)] f(\mathbf{p}', \mathbf{R}, t), \quad (1)$$

where the quantum distribution $f(\mathbf{p}, \mathbf{R}, t)$ is expressed in terms of a Schrödinger wave function, $\psi_\alpha(\mathbf{R}, t)$, which is characterized by a probability p_α satisfying $\sum_{\alpha=1}^N p_\alpha = 1$:

$$f(\mathbf{p}, \mathbf{R}, t) = \sum_{\alpha=1}^N p_\alpha \int \frac{d\mathbf{p}}{(2\pi\hbar)^3} \exp\left(\frac{i\mathbf{p} \cdot \mathbf{r}}{\hbar}\right) \times \psi_\alpha^*(\mathbf{R} + \mathbf{r}/2, t)\psi_\alpha(\mathbf{R} - \mathbf{r}/2, t). \quad (2)$$

Here U_{eff} is the potential field. Combined with Poisson's equation in integral form

$$U_{\text{eff}}(\mathbf{R}, t) = U(\mathbf{R}, t) + \int d\mathbf{R}' V(\mathbf{R} - \mathbf{R}') \times \int \frac{d\mathbf{p}'}{(2\pi\hbar)^3} f(\mathbf{p}', \mathbf{R}, t), \quad (3)$$

where V represents the Coulomb interaction, one obtains the linear longitudinal dielectric function

$$\epsilon(\mathbf{k}, \omega) = 1 + u_{\mathbf{k}} \sum_s \chi_s(\mathbf{k}, \omega), \quad (4)$$

where $u_{\mathbf{k}} = 4\pi e^2/k^2$ the Fourier components of $V(\mathbf{R})$ and χ_s the density response to the electric field in the form [14,15]

$$\chi_s^c(\omega, \mathbf{k}) = \int d^3 v \frac{\mathbf{k} \cdot \partial f_s/\partial v}{\omega - \mathbf{k} \cdot \mathbf{v}}, \quad (5)$$

$$\chi_s^q(\omega, \mathbf{k}) = \int \frac{d\mathbf{p}}{(2\pi)^3} \frac{f_{s,\mathbf{p}-\frac{1}{2}\mathbf{k}} - f_{s,\mathbf{p}+\frac{1}{2}\mathbf{k}}}{\omega - \hbar \mathbf{k} \cdot \mathbf{p}/m} \quad (6)$$

under classical and quantum conditions, respectively. Comparing Eqs. (5) and (6), the quantum density response can be reduced to the classical in the long-wavelength approxima-

tion. In the high damping region, the wave decays rapidly and does not contribute to transport. Therefore, it is appropriate to apply the weakly damped approximation when analyzing transport properties.

In the low temperature limit the Fermi distribution reduces to a step function and the real and imaginary parts of the density response become

$$\text{Re}\left(\chi_s^q\right) = \frac{mk_{\text{F}}}{2\pi^2\hbar} \left\{ 1 - \frac{1}{2\tilde{k}} \left[1 - \left(\frac{\tilde{\omega}}{\tilde{k}} - \frac{\tilde{k}}{2}\right)^2 \right] \ln\left|\frac{1 + \left(\frac{\tilde{\omega}}{\tilde{k}} - \frac{\tilde{k}}{2}\right)}{1 - \left(\frac{\tilde{\omega}}{\tilde{k}} - \frac{\tilde{k}}{2}\right)}\right| \right.$$
$$\left. + \frac{1}{2\tilde{k}} \left[1 - \left(\frac{\tilde{\omega}}{\tilde{k}} + \frac{\tilde{k}}{2}\right)^2 \right] \ln\left|\frac{1 + \left(\frac{\tilde{\omega}}{\tilde{k}} + \frac{\tilde{k}}{2}\right)}{1 - \left(\frac{\tilde{\omega}}{\tilde{k}} + \frac{\tilde{k}}{2}\right)}\right| \right\} \quad (7)$$

$$\text{Im}(\chi_s^q) = \begin{cases} -\frac{mk_{\text{F}}}{\hbar^2} \frac{1}{4\pi\tilde{k}} 2\tilde{\omega}, & \text{with } (\tilde{\omega}/\tilde{k} + \tilde{k}/2) < 1, \\ -\frac{mk_{\text{F}}}{\hbar^2} \frac{1}{4\pi\tilde{k}} \left[1 + \left(\frac{\tilde{\omega}}{\tilde{k}} - \frac{\tilde{k}}{2}\right)^2 \right], & \text{with } |\tilde{\omega}/\tilde{k} - \tilde{k}/2| < 1 < (\tilde{\omega}/\tilde{k} + \tilde{k}/2), \\ 0, & \text{with } |\tilde{\omega}/\tilde{k} - \tilde{k}/2| > 1. \end{cases}$$

Here $\tilde{\omega} = \omega/(\hbar k_{\text{F}}^2/m)$ is the normalized frequency and $\tilde{k} = k/k_{\text{F}}$ is the normalized wave number [31]. In the limit $\tilde{\omega} \gg \tilde{k}$, like for Langmuir waves in classical plasmas, we get the

dispersion relation [34]

$$\omega_{\text{LW}}(k) = \left(\omega_{\text{p}}^2 + \langle v^2 \rangle k^2 + \frac{\hbar^2 k^4}{4m_{\text{e}}^2}\right)^{1/2}. \quad (8)$$

For degenerate fermions, one has, of course,

$$\langle v^2 \rangle = \frac{3}{5}\left(\frac{p_{\mathrm{F}}}{m}\right)^2, \tag{9}$$

with $p_{\mathrm{F}} = \hbar k_{\mathrm{F}} = \hbar(3\pi^2 n)^{1/3}$ the Fermi momentum.

B. Quantum hydrodynamics

Quantum hydrodynamics equations trivially follows the Wigner-Poisson equations

$$\frac{\partial n}{\partial t} + \nabla \cdot (n\mathbf{u}) = 0, \tag{10}$$

$$\frac{\partial \mathbf{u}}{\partial t} + \mathbf{u} \cdot \nabla \mathbf{u} = \frac{e}{m}\nabla\Phi - \frac{1}{mn}\nabla\mathbf{P}, \tag{11}$$

with definitions of the density, velocity, and pressure [21]

$$n = \int \frac{d\mathbf{p}}{(2\pi\hbar)^3} f(\mathbf{p}, \mathbf{R}, t), \tag{12}$$

$$\mathbf{u} = \frac{1}{nm}\int \frac{d\mathbf{p}}{(2\pi\hbar)^3}\mathbf{p}f(\mathbf{p}, \mathbf{R}, t), \tag{13}$$

$$\mathbf{P} = m\int \frac{d\mathbf{p}}{(2\pi\hbar)^3}(\mathbf{v}^2 - \mathbf{u}^2)f(\mathbf{p}, \mathbf{R}, t). \tag{14}$$

The pressure can be separated into classical and quantum parts. The second of which can be written as

$$\mathbf{P}^{\mathrm{Q}} = -\frac{\hbar^2}{2m}[(\nabla\sqrt{n})^2 - \sqrt{n}\nabla^2\sqrt{n}] \tag{15}$$

whose gradient divided by particle density, $-\nabla\mathbf{P}^{\mathrm{Q}}/n = -\hbar^2\nabla(\nabla^2\sqrt{n}/2m\sqrt{n})$, is the Madelung term [35], and $W_{\mathrm{B}} = -\hbar^2\nabla^2\sqrt{n}/2m\sqrt{n}$ is the Bohm potential [14,15].

Linearizing in the long-wavelength range, we obtain the linear classical and quantum unified dispersion relation of Langmuir waves Eq. (8).

C. Two-stream instability in QHD

Studying collective effects such as fast ignition and white dwarfs in the quantum regime, we are interested in two-stream instabilities.

Ignoring kinetic effects and adopting the QHD approach [24], we have in this case

$$1 - \frac{\omega_{\mathrm{p}e}^2}{(\omega + \mathbf{k} \cdot \mathbf{u}_0)^2 - \omega_{\mathrm{u}}^2} - \frac{\omega_{\mathrm{be}}^2}{(\omega - \mathbf{k} \cdot \mathbf{u}_0)^2 - \omega_{\mathrm{u}}^2} = 0, \tag{16}$$

where $\omega_{\mathrm{pe}} = \omega_{\mathrm{be}} = \omega_{\mathrm{p}}$ for the two-stream case. The different considerations lead to different values of ω_{u}: (1) the classical zero temperature case, $\omega_{\mathrm{u}}^2 = 0$; (2) the classical Fermi distribution case, $\omega_{\mathrm{u}}^2 = \langle v^2 \rangle k^2$ with $\langle v^2 \rangle = (3/5)v_{\mathrm{F}}^2$; and (3) the quantum condition, $\omega_{\mathrm{u}}^2 = \langle v^2 \rangle k^2 + \hbar^2 k^4/4m_{\mathrm{e}}^2$. As expected, the expression of the dispersion relation is also naturally consistent with the QKT Langmuir wave under the long-wavelength approximation. Now we can expand the expression into polynomial form $(\omega^2 + k^2 u_0^2 - \omega_{\mathrm{u}}^2)^2 - 4k^2 u_0^2\omega^2 - 2(\omega^2 + k^2 u_0^2 - \omega_{\mathrm{u}}^2)\omega_p^2 = 0$. Then we obtain the solution

$$\omega^2 = \omega_{\mathrm{p}}^2 + \omega_{\mathrm{u}}^2 + k^2 u_0^2 \pm \left[\omega_{\mathrm{p}}^4 + 4k^2 u_0^2\left(\omega_{\mathrm{p}}^2 + \omega_{\mathrm{u}}^2\right)\right]^{1/2}. \tag{17}$$

It has two branches, one is a stable solution with $\omega^2 > 0$ and the other is an unstable solution with $\omega^2 < 0$. The unstable
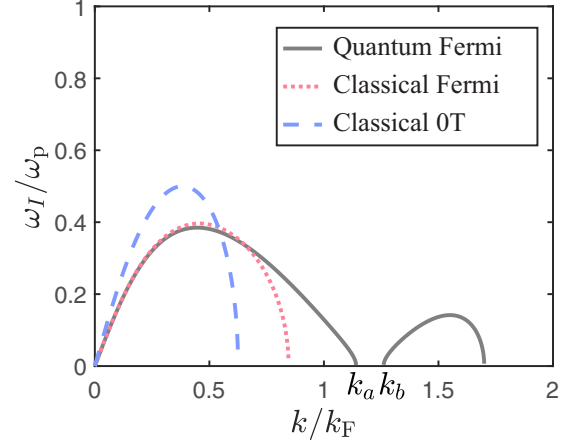

FIG. 1. Growth rates of different conditions at countering drift $u_0 = 1.15v_{\mathrm{F}}$, with parameters $T_{\mathrm{e}} = 0$ and $n_{\mathrm{p}} = n_{\mathrm{b}} = 10^{24}\mathrm{cm}^{-3}$.

solution satisfies

$$\left(k^2 u_0^2 - \omega_{\mathrm{u}}^2\right)\left(2\omega_{\mathrm{p}}^2 + \omega_{\mathrm{u}}^2 - k^2 u_0^2\right) < 0. \tag{18}$$

(1) In the classical zero temperature case, $\omega_{\mathrm{u}}^2 = 0$, instability region always exists. The unstable wave number interval is $k < \sqrt{2}\omega_{\mathrm{p}}/u_0$.

(2) For the classical Fermi distribution, we have $\omega_{\mathrm{u}}^2 = \langle v^2 \rangle k^2$. In this case, there is an instability threshold $u_0^2 > \langle v^2 \rangle$. The two-stream instability emerges when the countering drift velocity exceeds the thermal velocity [36,37]. The unstable region satisfies $k < \sqrt{2}\omega_{\mathrm{p}}/(u_0^2 - \langle v^2 \rangle)^{1/2}$.

(3) Under quantum conditions, we have $\omega_{\mathrm{u}}^2 = \langle v^2 \rangle k^2 + \hbar^2 k^4/4m_{\mathrm{e}}^2$. The threshold is the same as in the second case, $u_0^2 > \langle v^2 \rangle$. When $\langle v^2 \rangle < u_0^2 < \langle v^2 \rangle + \sqrt{2}\hbar\omega_{\mathrm{p}}/m$, the instability region satisfies $k < 2mU^{1/2}/\hbar$ where $U = u_0^2 - \langle v^2 \rangle$. When $u_0^2 > \langle v^2 \rangle + \sqrt{2}\hbar\omega_{\mathrm{p}}/m$, a new stable region $[k_a, k_b]$ appears:

$$k_{a,b}^2 = (2m^2/\hbar^2)\left[U \pm \left(U^2 - 2\hbar^2\omega_{\mathrm{p}}^2/m^2\right)^{1/2}\right]. \tag{19}$$

At zero temperature $U = v_0^2 - 3/5v_{\mathrm{F}}^2$.

Figure 1 shows that the effects of temperature or Fermi distribution enlarge the area of two-stream instability, while the maximum growth rate decreases. Comparing the second and third cases, we find that quantum correction expands the instability interval and simultaneously forms a new stable region in it, thereby splitting it into two growth intervals.

III. LANDAU DAMPING

In this section, we compare the quantum Landau damping with both QKT and QHD theories. QHD is a fluid theory which ignores the wave-particle interactions. In comparison, QKT is a more complete theory.

According to Eq. (8), when compared with the dispersion relation of classical Langmiur waves, $\omega(k) = (\omega_{\mathrm{p}}^2 + \langle v_{\mathrm{th}}^2 \rangle k^2)^{1/2}$, the Fermi distribution, promotes particles to fill the lowest energy levels and provides the system a minimum average kinetic energy. For this reason, there is no absolute "cold" plasma at low temperature limits. There is another
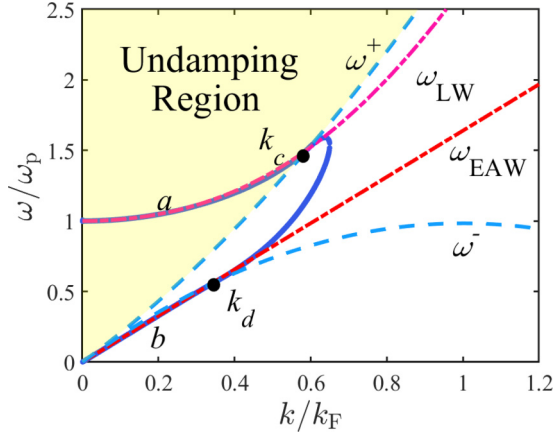
FIG. 2. Real dispersion relation of longitudinal oscillations of a degenerate electron gas by QKT with $T_e = 0$ and $n_e = 10^{24} \text{cm}^{-3}$. Here a is the optical mode and b is the acoustic mode. k_c and k_d represent, respectively, damping turning points of two modes. $\omega^{\pm} = \hbar k / 2m (2k_F \pm k)$ is the kinetic resonance frequency for particles on Fermi sphere [20].

wave structure called electron acoustic wave (EAW), which is certainly nonlinear and strongly damped, but can still exist in a plasma. In a classical plasma [38], its frequency is $\omega = 1.31 k v_{\text{th}}$ for small k, which is related to thermal pressure. Therefore, EAWs will not disappear at low temperature conditions, which is different from the classical plasmas.

Consider the limit that $\tilde{k}$ ($\tilde{k} > 0$) approach zero and $\tilde{\omega}/\tilde{k}$ has a finite value. According to the approximation $\ln|1 - (\frac{\tilde{\omega}}{\tilde{k}} \pm \frac{\tilde{k}}{2})| \approx \ln|1 - \frac{\tilde{\omega}}{\tilde{k}}| \pm \frac{\tilde{k}}{2|1-\frac{\tilde{\omega}}{\tilde{k}}|} + O(\tilde{k}^2)$, we expand the real part of Eq. (7), and the $\tilde{\omega}/\tilde{k}$ relation of quantum electron acoustic waves satisfies

$$-\frac{\tilde{\omega}}{\tilde{k}} \ln \left| \frac{1 + \frac{\tilde{\omega}}{\tilde{k}}}{1 - \frac{\tilde{\omega}}{\tilde{k}}} \right| + 2 = 0. \qquad (20)$$

The dispersion relation of EAWs under quantum conditions is $\omega_{\text{EAW}} \approx 0.834 k v_F$.

Using Eqs. (7) and (8), we can get the real solution of dispersion relation and obtain the weak damping rates

$$\gamma = -\epsilon_I(k, \omega_R)/(\partial \epsilon_R / \partial \omega)_{\omega_R}. \qquad (21)$$

Figure 2 shows the resonance curve $\omega^+(k)$ in the $\omega - k$ plane. For the waves whose phase velocity is greater than Fermi velocity, there are no particles satisfying the velocity condition and hence no particle can resonance with waves and contribute to Landau damping. The intersection of the optical mode and resonance curve $\omega^+(k)$ indicates a turning point k_c which shows Landau damping occurs for the part $k > k_c$ of the optical mode. Another turning point k_d exists at the intersection of the acoustic mode and resonance curve $\omega^-(k)$. However, unlike the optical mode, the acoustic mode is always damped.

Let us consider the influence of electron density on dispersion relation of the degenerate system. As shown in the Fig. 3, it is obvious that the optical mode approaches the classical electron Langmuir waves as density decreases. Another important point is that the acoustic mode approaches the k axis simultaneously and deviates from the kinetic resonance frequency (ω^-), which is consistence with the classical condition at low density limit.

The dissipative undamping region limit k_c of the optical mode is a parameter which shows the difference between quantum condition and classical condition. The formation of the undamping region is due to the steep edge of the Fermi-Dirac distribution [20], which is different from the undamping region based on Debye shielding at classical condition. The normalized kinetic resonance frequency is

$$\frac{\omega^{\pm}}{\omega_p} = \frac{\hbar k_F^2}{2m\omega_p} \left(2\frac{k}{k_F} \pm \frac{k^2}{k_F^2} \right) = \frac{\epsilon_F}{\hbar \omega_p} \left(2\frac{k}{k_F} \pm \frac{k^2}{k_F^2} \right), \qquad (22)$$

which can be derived from the imaginary part of Eq. (7).

According to Eqs. (8) and (22), the undamping limit k_c satisfies

$$\frac{k_c^3}{k_F^3} + \frac{2}{5} \frac{k_c^2}{k_F^2} - \frac{\hbar^2 \omega_{pe}^2}{\epsilon_F^2} = 0. \qquad (23)$$

As shown in Fig. 4(b), the first-order slope of resonance curve $\epsilon_F/\hbar \omega_p$ increases with density, which means the area
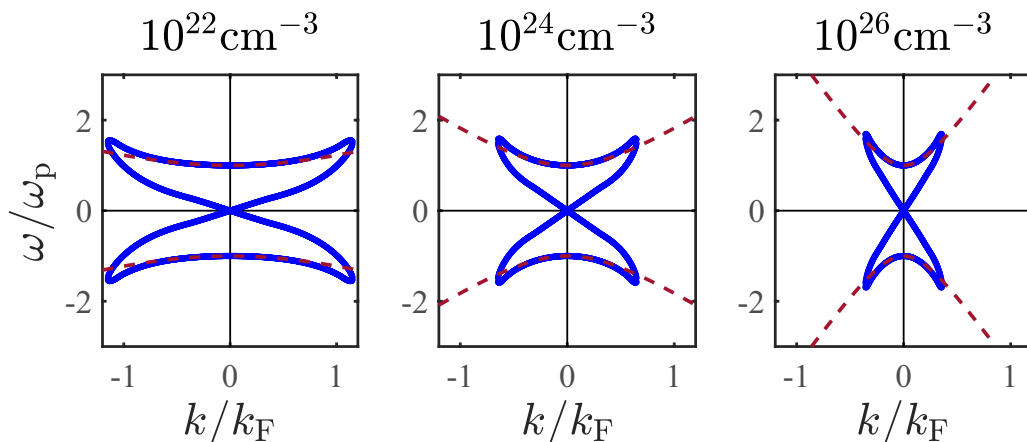

FIG. 3. The real part of longitudinal dispersion relation as the density changes shown by the solid lines (blue). The dashed lines represent the theoretical approach of optical mode $\omega_{\text{LW}}(k)$ (red).
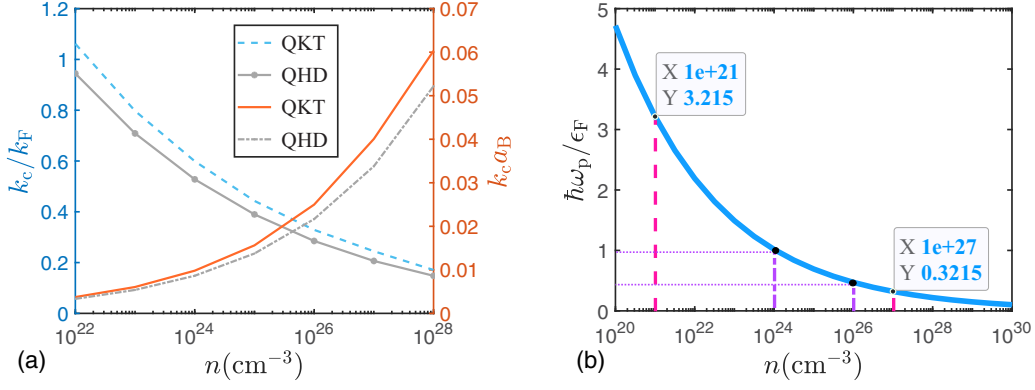
FIG. 4. (a) Various values of quantum undamping region limit k_c of optical mode with $T_e = 0$ as the density changes using QKT and QHD. Here, $a_B = 52.9$ pm is the hydrogen Bohr radius. (b) The ratio of plasmon energy and Fermi energy of degenerate system decreases as the density increases. In the density range of WDM, $10^{21} \sim 10^{27}$ cm^{-3} we can find the ratio is between 3.2 and 0.32. And in the density range of ICF, $10^{24} \sim 10^{26}$ cm^{-3}, the ratio is between 1 and 0.45.

of undamping region in the $\omega - k$ plane decreases simultaneously. The tendency of curve $k_c(n)$ also represents the same conclusion. It should be noted that the absolute value of k_c increases with density in the contrary because the Fermi wave vector k_F is proportional to $n^{1/3}$, shown by the solid line in Fig. 4(a).

The low temperature limit theory has pointed out some difference between the classical and quantum conditions, however, we cannot obtain an accurate result at finite temperature. Hence we can directly solve Eq. (6) by using small damping approximation from the beginning. The real part of the dispersion relation can only be given analytically at some limiting cases [39,40]. The imaginary part can be found by the theoretical approach

$$\text{Im}\left(\chi_s^q(\omega, k)\right) = \frac{2e^2 m^2}{\beta k^3 \hbar^4} \ln\left(\frac{\tilde{f}_-(\omega, k)}{\tilde{f}_+(\omega, k)}\right), \qquad (24)$$

where

$$\tilde{f}_\pm(\omega, k) = 1 + \exp\left[\mu\beta - \left(\frac{\omega}{k} \pm \frac{k}{2}\right)^2 \frac{\beta}{2m}\right]. \qquad (25)$$

The parameter μ and β in the above equation represent, respectively, the chemical potential and temperature of the system. Hence we can use Eq. (21) and the real part solutions to obtain the damping rates.

We plot the real part of the dispersion relation in Fig. 5. High temperatures break the steep edge of the Fermi distribution and narrow the difference between quantum theory and the classical limit. For this reason, the undamping region will disappear. However, at relatively low temperature, there are very few particles with large momentum which can resonate with waves. Hence, just like what we implemented at the low temperature limit case, here we have $2/(e^{\beta(\hbar^2 k_t^2/2m - \mu)} + 1) > 1/n$ where the factor of 2 stands for the spin. Then we get $k_t^2 = 2m/\hbar^2[\mu + \frac{1}{\beta} \ln(2n)]$.

Replacing k_F at low temperature with k_t, and accounting for energy conservation, we have the approximate resonance

frequency for particles at finite temperature:

$$\omega_\pm = k\sqrt{\frac{2}{m}\left(\mu + \frac{1}{\beta}\ln(2n)\right)} \pm \frac{\hbar k^2}{2m}. \qquad (26)$$

Then we can determine the undamping region limit k_c according to the intersection of the resonance frequency curve and Langmuir wave curve Eq. (8), shown by the dashed line in Fig. 5.

The tendency of the two curves in Fig. 6 is basically the same. Therefore, the reason for the formation of dissipative undamping region is indeed the particularity of Fermi distribution. As shown in the figure, the value of k_c/k_F tends to zero as temperature increases. It means at the high temperature limit, since the Fermi distribution is equivalent to the Maxwellian, the undamping region disappears, which is consistent with the classical situation.

IV. TWO-STREAM INSTABILITY

In this section, we compare the two-stream instability in QKT and QHD. To maintain symmetry, we study the nonrelativistic countering-stream, which can also be obtained from
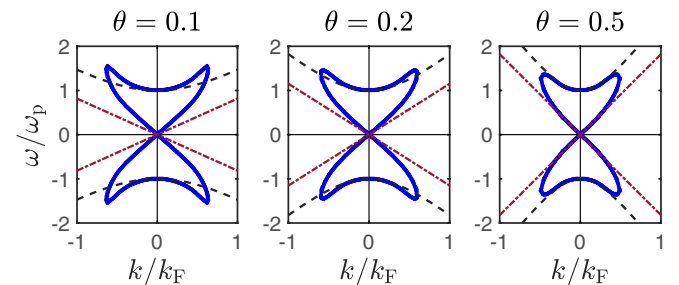

FIG. 5. The solid lines (blue) represent the real part of dispersion relation as the temperature $\theta = k_B T/\epsilon_F$ changes. The dashed line (gray) is classical Langmuir waves $\omega = (\omega_p^2 + \langle v_{th}^2 \rangle k^2)^{1/2}$. The dotted line (red) is classical EAWs $\omega = 1.31 k v_{th}$ [38].
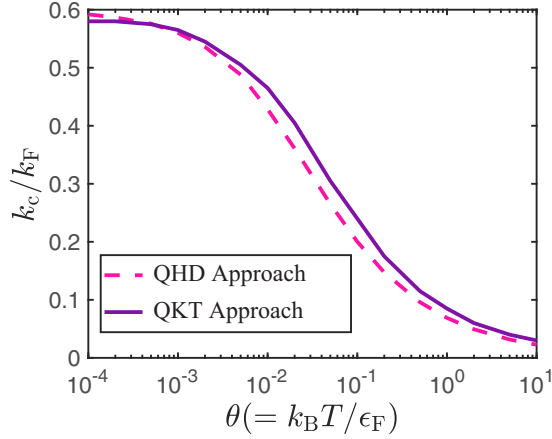
FIG. 6. The undamping region limit of optical mode ($n = 10^{24}$ cm^{-3}) at finite temperature according to the approximate resonance condition is shown by the dashed line. The solid line represents the theoretical approach of imaginary part of dielectric function.

the two-stream case by coordinate transformation

$$\epsilon(\mathbf{k}, \omega) = 1 + u_{\mathbf{k}} \chi_{pe}(\mathbf{k}, \omega + \mathbf{k} \cdot \mathbf{u_0}) + u_{\mathbf{k}} \chi_{be}(\mathbf{k}, \omega - \mathbf{k} \cdot \mathbf{u_0}), \quad (27)$$

where χ_{pe} and χ_{be} are the susceptibilities of background and beam, respectively.

Now we can add the previously omitted kinetic Landau damping to the theoretical results of QHD. Due to the existence of two parts of countering stream electrons, their respective undamped regions will overlap. When the countering stream speed exceeds a certain threshold, the overlap forms a new dissipative undamping region.

In Fig. 7, the increase in countering-stream velocity causes the new undamping region to expand, until completely covering the first growth interval of two-stream instability. According to the intersection of two kinetic resonance frequency curves $\omega^+ - \mathbf{k} \cdot \mathbf{u_0} = \omega^- + \mathbf{k} \cdot \mathbf{u_0}$, we have the vertex of a new dissipative undamping region:

$$k = 2(mu_0/\hbar - k_{\text{F}}). \quad (28)$$

This stable region also coincides with part or all of the two-stream instability growth region. Combing Eqs. (19) and (28), we get the countering stream velocity for covering the dissipative undamping region and growth regions

$$\frac{u_{\text{c}}^2}{v_{\text{F}}^2} + \frac{13}{5} - 4\frac{u_{\text{c}}}{v_{\text{F}}} + \sqrt{\left(\frac{u_{\text{c}}^2}{v_{\text{F}}^2} - \frac{3}{5}\right)^2 - \frac{1}{2}\frac{\hbar^2 \omega_{\text{p}}^2}{\epsilon_{\text{F}}^2}} = 0. \quad (29)$$

Figure 8 shows that as the density increases, the ratio of threshold to Fermi velocity decreases, while the absolute value increases, which is consistent with the trend of k_{c} in Sec. II.

When the countering stream velocity is greater than the threshold, the instability of this region appears as a pure two-stream growth rate without Landau damping. From the perspective of the distribution function, when the phase velocity of waves is located at the "gap" between two parts of the distribution, waves can become directly excited without Landau damping.
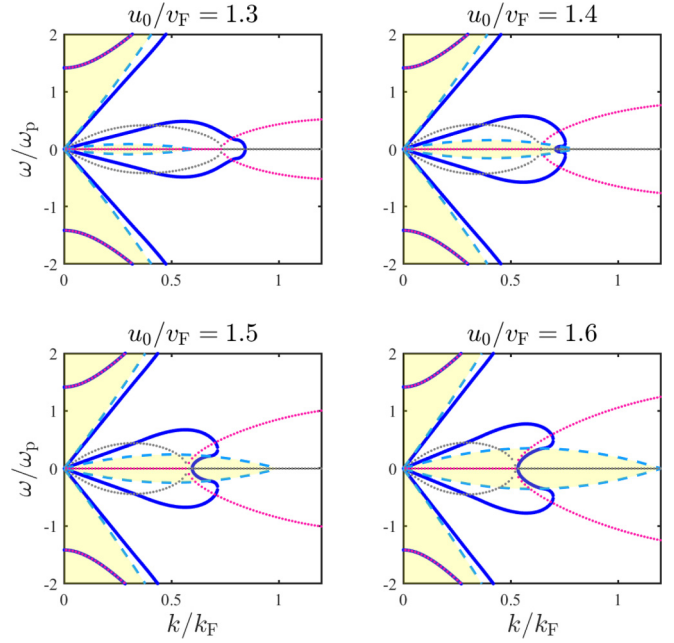

FIG. 7. The same as Fig. 2, but for countering-stream case ($T_e = 0$, $n_{\text{p}} = n_{\text{b}} = 10^{24}$ cm^{-3}). Solid lines (blue) represent the numerical solution of QKT, and dotted lines represent the real (red) and imaginary (gray) solution of QHD. The enclosed dashed curves (light blue) form a new dissipative undamping region.

As the countering stream velocity increases, the results of QHD and QKT gradually coincide. When the stable mode appears in QKT ($u_0 \approx u_{\text{c}}$), the differences between the two theories are relatively large because the approximation of QHD is invalid in the short-wavelength region.

Quantum corrections (Fermi-Dirac distribution and quantum diffraction) are the reason for the formation of this new dissipative stable region. Considering the dispersion relation of the Fermi system in the classical case, ignoring the k^2 term which represents the quantum wave effect, we have the resonance curve function which can be expressed as a linear function from Eq. (22). Hence we find that the similar stable region is an open interval composed of two rays in the
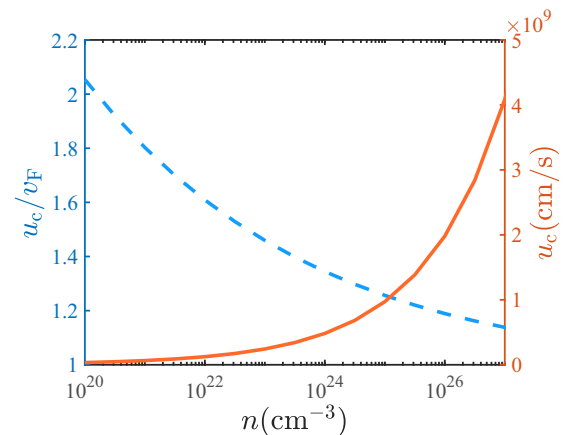

FIG. 8. the value of countering velocity threshold with the change of electron density.
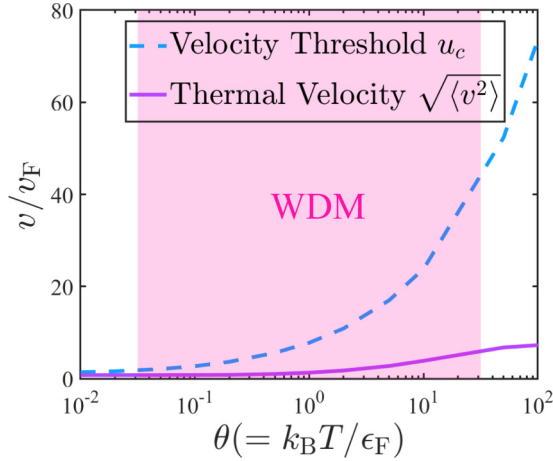
FIG. 9. The value of countering stream velocity threshold with the change of temperature ($n = 10^{24}$ cm^{-3}).

classical case, which is different from the closed interval in the quantum case. Thus, when $u_0/v_F > 1$, the entire range of two-stream instability is completely within this region in the classical case.

Therefore, in the quantum case, within a certain countering velocity range, the wave growth rate is the result of the combined effect of two-stream instability and wave-particle resonance, which cannot be considered separately.

In Sec. II, we mentioned that the increase in temperature will lead to the reduction of undamping region, which is consistent with classical case at high temperature limit. According to Eqs. (26) and (19), we can obtain the vertex of the undamping region

$$k = \frac{2m}{\hbar}\left(u_0 - \sqrt{\frac{2}{m}\left(\mu + \frac{1}{\beta}\ln(2n)\right)}\right) = \frac{2m}{\hbar}(u_0 - v_\mu).$$

(30)

Similarly, we can obtain the countering-stream velocity threshold where dissipative undamping coincides with the first growth region of two-stream instability

$$u_c^2 - 4v_\mu u_c + 2v_\mu^2 + \langle v^2 \rangle + \sqrt{\left(u_c^2 - \langle v^2 \rangle\right)^2 - \frac{2\hbar^2 \omega_p^2}{m^2}} = 0.$$

(31)

When we plot the solution of Eq. (31) in Fig. 9, we can see that as temperature increases, the equivalent thermal velocity is also increasing, which means that a higher velocity is required to cause the appearance of two-stream instability. The

threshold velocity rises faster, which means that the higher the system temperature, the higher the countering velocity is needed to make two-stream instability completely free of Landau damping. However, a high countering velocity will cause two-stream instability to be insignificant, and simultaneously the theory of relativity needs to be considered, which also requires the basic model to be revised. Therefore, in the high temperature region, two-stream instability is bound to be accompanied by a certain Landau damping.

V. CONCLUSION

We discussed the quantum effect of two-stream instability in high energy density plasmas by means of quantum kinetic theory and quantum hydrodynamics. The discrepancies of these two theoretical frameworks are caused by wave-particle interaction, i.e., kinetic effects, which is ignored by QHD. We conclude that, first, the Fermi statistic effect yields a stable region without Landau damping, which is further deformed by the single-particle Bohm potential. The stable region shrinks as the temperature rises, which means the quantum effect is being concealed by the thermal effect. Second, the unstable region of two-stream instability is split into two parts by the Bohm effect, one of which is located at the dissipative undamping region, thus yielding a pure two-stream instability growth region. Last but not least, there exists a threshold drift velocity beyond which the two-stream instability decouples with Landau damping and becomes a pure fluid instability. This threshold also increases as temperature rises.

The findings in this paper can have major implications on the beam stopping by the warm dense background plasmas, especially in inertial confinement fusion research [6–8]. Compared with the classical case, quantum two-stream instability has a larger regime so that it is easier for the beam to excite Langmuir waves and cause stronger beam stopping. On the contrary, Landau damping can inhibit the excitation of Langmuir waves to reduce beam stopping. Especially in the WDM regime, the high countering stream velocity threshold implies that these two mechanisms are coupled and simultaneously affect the actual beam stopping.

[1] T. G. White, N. J. Hartley, B. Borm, B. J. B. Crowley, J. W. O. Harris, D. C. Hochhaus, T. Kaempfer, K. Li, P. Neumayer, and L. K. Pattison, Electron-ion Equilibration in Ultrafast Heated Graphite, Phys. Rev. Lett. **112**, 145005 (2014).

[2] A. Pelka, G. Gregori, D. O. Gericke, J. Vorberger, S. H. Glenzer, M. M. Günther, K. Harres, R. Heathcote, A. L. Kritcher, and

N. L. Kugland, Ultrafast Melting of Carbon Induced by Intense Proton Beams, Phys. Rev. Lett. **105**, 265701 (2010).

[3] G. M. Dyer, A. C. Bernstein, B. I. Cho, J. Osterholz, and T. Ditmire, Equation-of-State Measurement of Dense Plasmas Heated with Fast Protons, Phys. Rev. Lett. **101**, 015002 (2008).

[4] J. Lindl, Development of the indirect-drive approach to inertial confinement fusion and the target physics basis for ignition and gain, Phys. Plasmas **2**, 3933 (1995).

[5] X. T. He, J. W. Li, Z. F. Fan, L. F. Wang, J. Liu, K. Lan, J. F. Wu, and W. H. Ye, A hybrid-drive nonisobaric-ignition scheme for inertial confinement fusion, Phys. Plasmas **23**, 082706 (2016).

[6] M. Tabak, J. Hammer, M. E. Glinsky, W. L. Kruer, and R. J. Mason, Ignition and high gain with ultrapowerful lasers*, Phys. Plasmas **1**, 1626 (1994).

[7] S. P. D. Mangles, C. D. Murphy, Z. Najmudin, A. G. R. Thomas, J. L. Collier, A. E. Dangor, E. J. Divall, P. S. Foster, J. G. Gallacher, and C. J. Hooker, Monoenergetic beams of relativistic electrons from intense laser-plasma interactions, Nature **431**, 535 (2004).

[8] M. Tatarakis, F. N. Beg, E. L. Clark, A. E. Dangor, R. D. Edwards, R. G. Evans, T. J. Goldsack, K. W. D. Ledingham, P. A. Norreys, and M. A. Sinclair, Propagation Instabilities of High-Intensity Laser-Produced Electron Beams, Phys. Rev. Lett. **90**, 175001 (2003).

[9] T. P. Fleming, J. M. Stone, and J. F. Hawley, The effect of resistivity on the nonlinear stage of the magnetorotational instability in accretion disks, Astrophys. J. **530**, 464 (2008).

[10] D. E. Innes, B. Inhester, W. I. Axford, and K. Wilhelm, Bidirectional plasma jets produced by magnetic reconnection on the sun, Nature **386**, 811 (1997).

[11] D. Biskamp, Magnetic reconnection via current sheets, Phys. Fluids **29**, 1520 (1986).

[12] L. D. Landau, On the vibrations of the electronic plasma, Zh. Eksp. Teor. Fiz. **16**, 574 (1946).

[13] F. F. Chen, *Introduction to Plasma Physics and Controlled Fusion*, Vol. 1 (Springer, New York, 1984).

[14] D. Pines and D. Bohm, A collective description of electron interactions: II. Collective vs individual particle aspects of the interactions, Phys. Rev. **85**, 338 (1952).

[15] D. Bohm and D. Pines, A collective description of electron interactions: III. coulomb interactions in a degenerate electron gas, Phys. Rev. **92**, 609 (1953).

[16] M. Bonitz, T. Dornheim, Zh. A. Moldabekov, S. Zhang, P. Hamann, A. Filinov, K. Ramakrishna, and J. Vorberger, *Ab initio* simulation of warm dense matter, Phys. Plamsas **27**, 042710 (2020).

[17] M. Bonitz, Zh. A. Moldabekov, and T. S. Ramazanov, Quantum hydrodynamics for plasmas–Quo vadis? Phys. Plasmas **26**, 090601 (2019).

[18] M. Bonitz, R. Binder, D. C. Scott, S. W. Koch, and D. Kremp, Theory of plasmons in quasi-one-dimensional degenerate plasmas, Phys. Rev. E **49**, 5535 (1994).

[19] M. Bonitz, *Quantum Kinetic Theory* (Springer, New York, 2016).

[20] S. V. Vladimirov and Yu O. Tyshetskiy, On description of a collisionless quantum plasma, Phys. Usp. **54**, 1243 (2011).

[21] G. Manfredi and F. Haas, Self-consistent fluid model for a quantum electron gas, Phys. Rev. B **64**, 075316 (2001).

[22] H. Ren, Z. Wu, J. Cao, and P. K. Chu, Dispersion of multistream instability in quantum magnetized hot plasmas, Phys. Lett. A **372**, 2676 (2008).

[23] F. Haas, G. Manfredi, and M. Feix, Multistream model for quantum plasmas, Phys. Rev. E **62**, 2763 (2000).

[24] F. Haas, *Quantum Plasmas* (Springer-Verlag, New York, 2011).

[25] F. Haas, Kinetic theory derivation of exchange-correlation in quantum plasma hydrodynamics, Plasma Phys. Controlled Fusion **61**, 044001 (2019).

[26] H.-J. Kull, Quantum two-stream instability with exchange interaction, J. Phys.: Conf. Ser. **826**, 012012 (2017).

[27] M. Akbari-Moghanjoughi, M. Mohammadnejad, and A. Esfandyari-Kalejahi, Electrostatic two-stream instability in fermi-dirac plasmas, Astrophys. Space Sci. **361**, 307 (2016).

[28] M. Akbari-Moghanjoughi, Hydrodynamic limit of wignerpoisson kinetic theory: Revisited, Phys. Plasmas **22**, 022103 (2015).

[29] M. Mohammadnejad and M. Akbari-Moghanjoughi, Two stream ion acoustic wave instability in warm dense plasmas, Astrophys. Space Sci. **364**, 23 (2019).

[30] S. Son, Two stream instabilities in degenerate quantum plasmas, Phys. Lett. A **378**, 2505 (2014).

[31] J. Lindhard, On the properties of a gas of charged particles, Matematisk-fysiske Meddelelser Kongelige Danske Videnskabernes Selskab **28**, 1 (1954).

[32] L. P. Kadanoff and G. Baym, *Quantum Statistical Mechanics* (W. A. Benjamin, New York, 1962).

[33] E. P. Wigner, On the quantum correction for thermodynamic equilibrium, Phys. Rev. **40**, 749 (1932).

[34] Y. L. Klimontovich and V. P. Silin, *o spektrakh sistem vzaimodeistvuyushchikh chastits, Zh. Eksp. Teor. Fiz. **23**, 151 (1952).

[35] E. Madelung, Quantum theory in hydrodynamic form, Z. Phys. **40**, 322 (1926).

[36] T. M. O'Neil and J. H. Malmberg, Transition of the dispersion roots from beam-type to Landau-type solutions, Phys. Fluids **11**, 1754 (1968).

[37] G. Francis, A. K. Ram, and A. Bers, Finite temperature effects on the space-time evolution of two-stream instabilities, Phys. Fluids **29**, 255 (1986).

[38] J. P. Holloway and J. J. Dorning, Undamped plasma waves, Phys. Rev. A **44**, 3856 (1991).

[39] I. I. Goldman, Oscillations of a degenerate electron fermi gas, Zh. Eksp. Teor. Fiz. **17**, 681 (1947).

[40] V. P. Silin, *k teorii spektra vozbuzhdenii sistemy mnogikh chastits, Zh. Eksp. Teor. Fiz. **23**, 641 (1952).